Electronic Supplementary Information

A resettable and reprogrammable biomolecular keypad lock with dual outputs based on glucose oxidase-Au nanoclusters-Prussian blue nanocomposite films on an electrode surface

Xue Yu,[a] Menglu Li,[a] Tianrui Li,[b] Shuo Zhou[b] and Hongyun Liu[*a]

[a] College of Chemistry, Beijing Normal University, Beijing 100875, People's Republic of China

[b] Beijing No.55 High School, Beijing 100027, People's Republic of China

*Corresponding author: Hongyun Liu, 19, Xinjiekouwai Street, Haidian District, Beijing 100875, People's Republic of China. Tel: (86)-10-58807843. E-mail: liuhongyun@bnu.edu.cn.
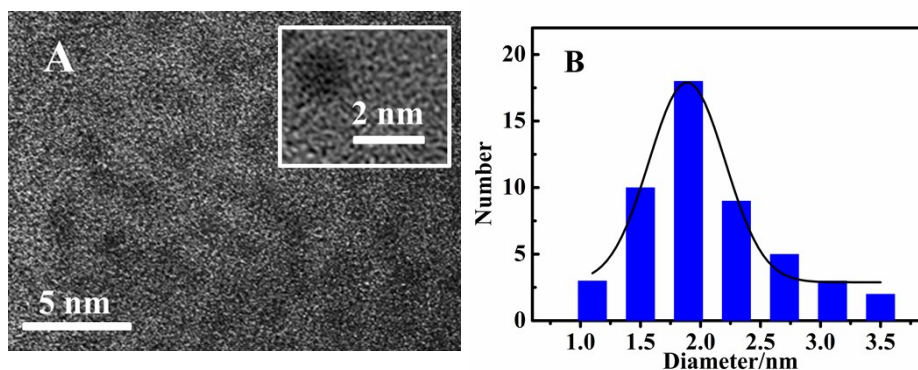
Fig. S1 (A) TEM image of AuNCs. (B) Size distribution of AuNCs obtained from analysis of counting 50 particles in the TEM image.
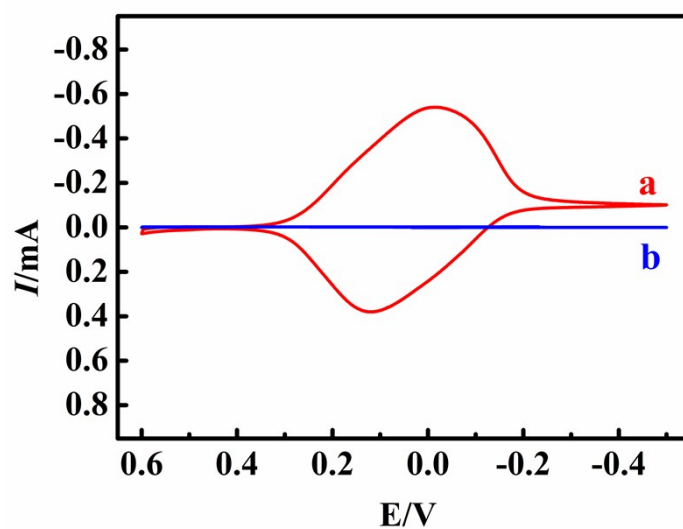

Fig. S2 CVs at 0.01 V s^{-1} in pH 6.0 buffers for (a) PB films at ITO electrodes and (b) bare ITO electrodes.
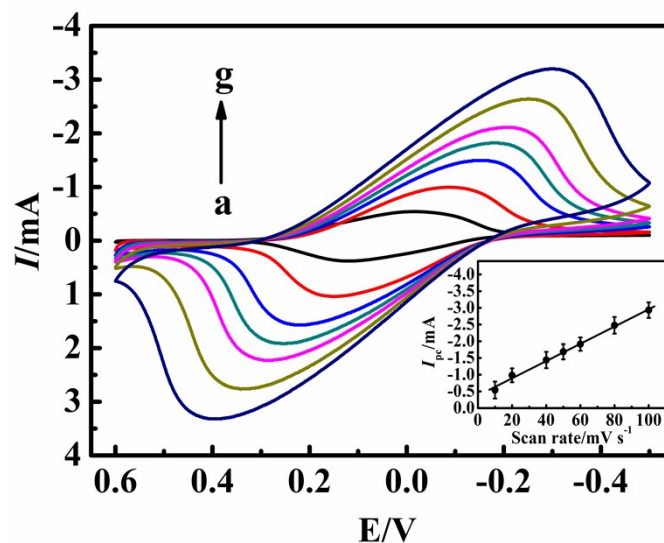
Fig. S3 CVs at different scan rates (a – g: 10, 20, 40, 50, 60, 80, 100 mV s^{-1}) of the PB film electrode in pH 6.0 buffers. Inset: the relationship between the CV reduction peak current (I_{pc}) and scan rates.
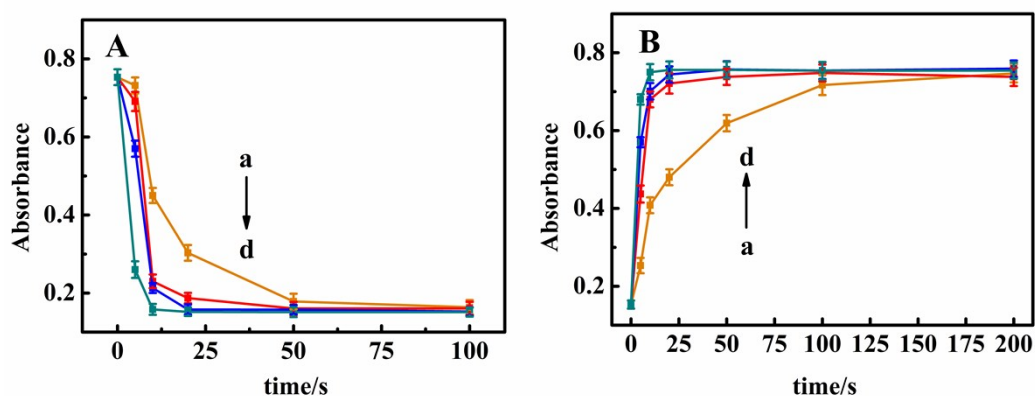

Fig. S4 (A) Dependence of UV-vis absorbance for CS-AuNCs-GOD/PB films in pH 6.0 buffers on the time of applying potential at (a) 0, (b) −0.1, (c) −0.2 and (d) −0.3 V. (B) Dependence of UV-vis absorbance for CS-AuNCs-GOD/PW films in pH 6.0 buffers on the time of applying potential at (a) 0.2, (b) 0.3, (c) 0.4 and (d) 0.5 V.
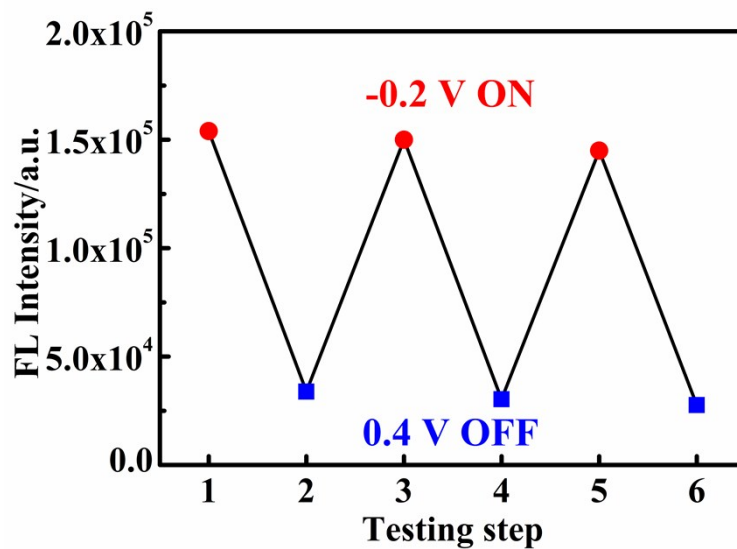
Fig. S5 Variation of fluorescence emission intensity at 616 nm with applied potential switched between 0.4 and −0.2 V for the nanocomposite film electrode in pH 6.0 buffers.
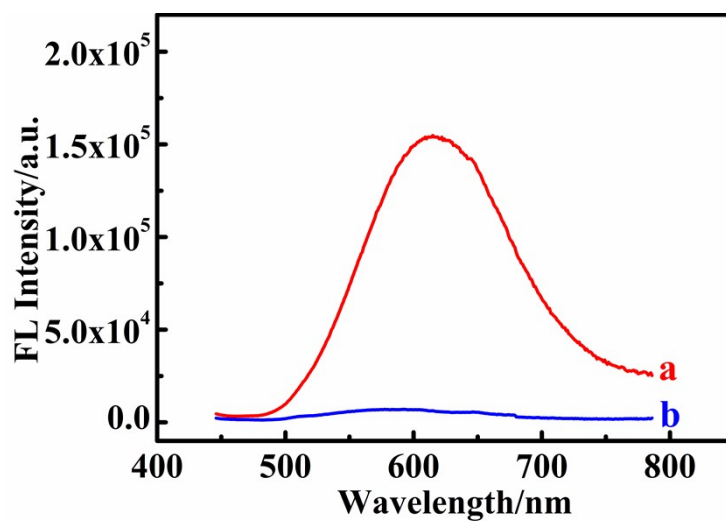

Fig. S6 Fluorescence emission spectra of (a) CS-AuNCs-GOD/PW and (b) AuNCs-GOD/PW film electrodes after −0.2 V was applied for 100 s in pH 6.0 buffers with excitation at 416 nm.
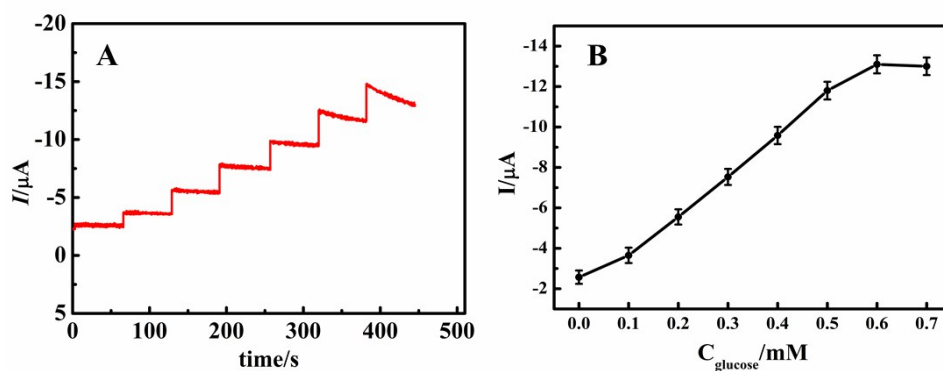
Fig. S7 (A) Amperometric responses at CS-AuNCs-GOD/PW film electrodes after successive addition of 0.1 mM glucose into pH 6.0 buffer solutions equilibrated with air at constant potential of −0.2 V. (B) The dependence of amperometric current at CS-AuNCs-GOD/PW film electrodes on the glucose concentration.
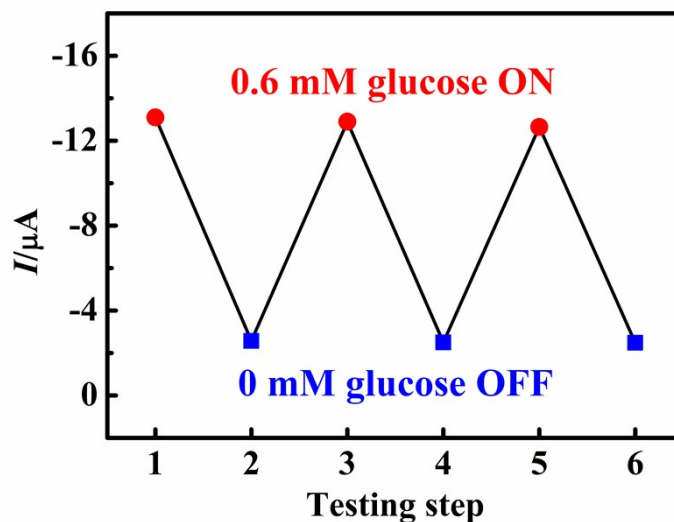

Fig. S8 Variation of amperometric currents at CS-AuNCs-GOD/PW film electrodes in pH 6.0 buffers equilibrated with air at constant potential of −0.2 V with switching the film electrode in solution between in the presence of 0.6 mM glucose and in the absence of glucose.

Table S1 Truth table of the 2-input/3-output logic gate for the system

Input A	Input B	Output A	Output B	Output C
potential	glucose	$|I|$	FL Intensity (616 nm)	A (700 nm)
1	1	1	0	1
1	0	0	1	0
0	1	0	0	1
0	0	0	0	1

A

Input A	Input B	Output B
potential	glucose	FL Intensity (616 nm)
1	0	1
0	1	0

B

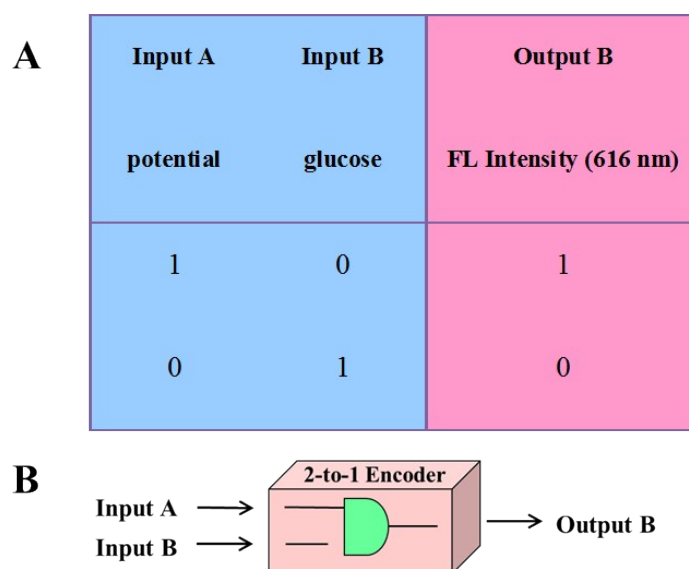2-to-1 Encoder

Input A →
Input B →
→ Output B

Fig. S9 (A) Truth table and (B) the symbolic representation of the 2-to-1 encoder with potential as Input A and glucose as Input B, and the fluorescence peak at 616 nm as Output B.

Table S2 The truth table for the keypad lock system

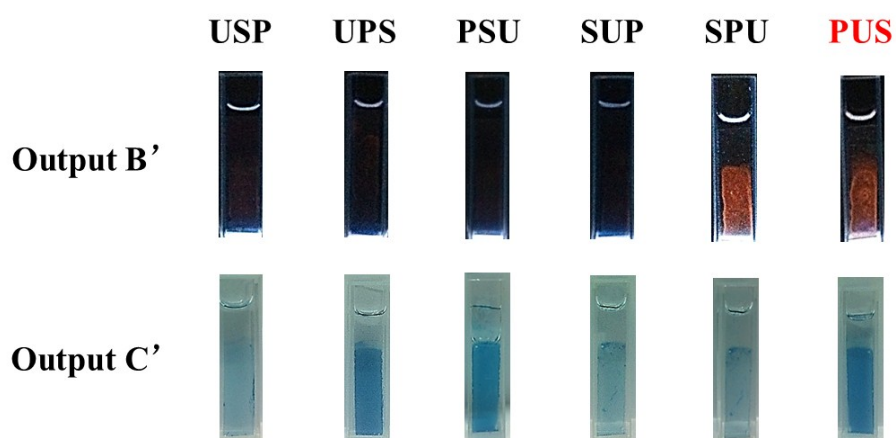| Input sequence			Output B	Output C
U	S	P	0	0
U	P	S	0	1
P	S	U	0	1
S	U	P	0	0
S	P	U	1	0
P	U	S	1	1

Fig. S10 Photographs of the nanocomposite film electrodes with 6 possible sequences of the 3 inputs for the keypad lock system taken under irradiation of the UV light at 365 nm (Output B') and after all the 3 input operations were finished (Output C').